RAMAN SCATTERING IN QUANTUM WIRE IN A MAGNETIC FIELD

T.G. ISMAILOV, B.H. MEHDIYEV
Institute of Physics of Azerbaijan National Academy of Sciences
Baku, Az-1143, H. Javid ave. 33

Electron Raman scattering are investigated in a parabolic semiconductor quantum wire in a transverse magnetic field neglecting phonon-assisted transitions. The ERS cross-section is calculated as a function of the frequency shift and the magnetic field strength. The process involves an interband electronic transition and an intraband transition between quantized subbands. We analyze the differential cross-section for different scattering configurations. We study selection rules for the processes. The singularities in the Raman spectra are found and interpreted. The scattering spectrum shows density-of-states peaks and interband matrix elements maximums and strong resonance when scattered frequency equals the "hybrid" frequency or confinement frequency depending on polarization. Numerical results are presented using parameters caaracteristic of GaAs/AlGaAs.

1. Introduction

Low-dimensional semiconductor systems, particularly quantum wires are attracting considerable attention recently, in part, because they exhibit novel physical properties and also because of potential applications involving them. In recent years, a number of innovative techniques have been developed to grow or to fabricate and to study experimentally a variety of quantum wire structures having different geometries and potentials.

Many recent experimental and theoretical studies have been performed on quantum wires subjected to a transverse magnetic field [1-7]. The electronic properties of quantum well wires in a transverse magnetic field have investigated in [8-9]. The subband dispersion and magnetoabsorption have been studied for rectangular QW in [10].

Magnetic field applied perpendicular to the wire axis, "free electron" direction, can change significantly the electronic states of semiconductor quantum wire structures.

Electron Raman scattering seems to be a useful technique providing direct information on the energy band structure and the optical properties of the investigated systems [11-12]. In particular, the electronic structure of semiconductor materials and nanostructures can be thoroughly investigated considering different polarizations for the incident and emitted radiation [13].

The differential cross-section in general case, usually shows singularities related to interbanda and interband transitions. This latter result strongly depends on the scattering configurations: the structure of the singularities is varied when the photon polarizations change. This feature of ERS allows to determine the subband structure of the system by direct inspection of the singularity positions in the spectra.

For bulk semiconductors ERS has been studied in the presence of external applied magnetic and electric fields[14-16]. In the case of a quantum well preliminary results were reported in [17]

Raman scattering in low-dimensional semiconductor systems has been the subject of many theoretical and experimental investigations [18, 19].

Interband ERS processes can be qualitatively described in the following way: after the absorption of an external photon from the incident radiation field a virtual electron-hole pair is created in an intermediate crystal state by means of an electron interband transition involving the crystal valence and conduction bands. The electron (hole) in the conduction (valence) band is subject to a second interband transition with the emission of secondary radiation photon. Therefore, in the final state we have a real electron-hole pair in the crystal and a photon of the secondary radiation field. The effect of external applied fields on this kind of processes for bulk semiconductors were investigated in [15, 16]. In the case of a quantum well preliminary results were reported in Ref. [17].

In this work we present a systematic study of the interband ERS in direct band gap semiconducting parabolic quantum wire in a transverse magnetic field. In these systems due to electron confinement and magnetic field the conduction (valence) band is split in a subband system and transitions between them determine the ERS processes. Numerical results for the ERS differential cross-section are presented using parameters characteristic of GaAs/AlGaAs.

This paper is organized as follows. In Section II the energy spectrum and wave functions for QW with parabolic confinement potential are given in a transverse magnetic field. In Section III we present the general relations needed for our calculations of the ERS cross-section. Section IV is devoted to the calculations of the ERS differential cross-sections. Finally Section V is concerned with the discussion of the obtained results.

2. Wave functions and energy spectrum

We consider a quantum wire aligned along the y direction with transverse magnetic field $\vec{H} = (0,0,H)$ applied along z direction. The quantum wire is characterized by parabolic confinements in the plane (x, z). The effective mass Schrodinger equation for electron in conduction band can be written as

$$\left(\frac{1}{2 \cdot m_e} \left(\vec{p} + \frac{e}{c} \vec{A} \right)^2 + \frac{1}{2} m_e \omega_{0e}^2 \left(x^2 + z^2 \right) \right) \psi_e(x, y, z) = E_e \psi_e(x, y, z) \tag{1}$$

where $\vec{A}=(0,Hx,0)$ the vector potential in the Landau gauge and ω_{0e} characterizes the parabolic potential of the QW for electron in conduction band. We look for the solution in the form $\psi_e(x,y,z)=\varphi(x)\eta(z)e^{\frac{i}{\hbar}p_{y,e}y}$ where $p_{y,e}=\hbar k_{y,e}$ is the quasi-momentum of an electron.

After trivial shifting of the origin of coordinates and separating the variables in the usual way we obtain the eigenfunctions and eigenvalues of the Schrödinger equation (1)

$$\psi_{N_{1e},N_{2e},k_{y,e}}=\varphi_{N_{1e}}\left(\frac{x-x_{0e}}{\widetilde{L}_e}\right)\eta_{N_{2e}}\left(\frac{z}{L_e}\right)e^{ik_{y,e}y} \tag{2}$$

$$E_e=\left(N_{1e}+\frac{1}{2}\right)\hbar\widetilde{\omega}_e+\left(N_{2e}+\frac{1}{2}\right)\hbar\omega_{0e}+\frac{\hbar^2k_{y,e}^2}{2m_e}\left(\frac{\omega_{0e}}{\widetilde{\omega}_e}\right)^2 \tag{2, a}$$

The wave functions and energy eigenvalues for electron in valence band can be written as

$$\psi_{N_{1h},N_{2h},k_{y,h}}=\varphi_{N1h}\left(\frac{x-x_{0h}}{\widetilde{L}_h}\right)\eta_{N_{2e}}\left(\frac{z}{L_h}\right)e^{ik_{y,h}y} \tag{3}$$

$$E_h=-E_g-\left(N_{1h}+\frac{1}{2}\right)\hbar\widetilde{\omega}_h-\left(N_{2h}+\frac{1}{2}\right)\hbar\omega_{0h}-\frac{\hbar^2k_{y,h}^2}{2m_h}\left(\frac{\omega_{0h}}{\widetilde{\omega}_h}\right)^2 \tag{3,a}$$

where E_g is the gap energy of the bottom of the conduction band in the absence of the external magnetic field, ω_{0h} oscillator frequency of the parabolic potential for electron in the valence band. In Eqs. (2) and (3)

$$\widetilde{\omega}_{e,h}=\sqrt{\omega_{0e(h)}^2+\omega_{e(h)}^2} \tag{4}$$

is "hybrid" frequency. The subscript e and h denote conduction and valence band electrons, respectively.

$$\omega_{e(h)}=\frac{eH}{m_{e(h)}c} \tag{5}$$

is the cyclotron frequency, $m_{e(h)}$ is the effective mass.

$$x_{0e(h)}=\frac{\hbar\omega_{e(h)}}{m_{e(h)}\widetilde{\omega}_{e(h)}^2}k_{ye(h)} \tag{6}$$

is oscillator centre.

The full energy spectrum in (2) and (3) is governed by quantum numbers $N_{1e(h)}$, $N_{2e(h}$ and $k_{ye(h)}$.

$$\varphi_{N_{1e(h)}}\left(\frac{x-x_{oe(h)}}{\widetilde{L}_{e(h)}}\right)=\left(\frac{1}{\pi\widetilde{L}_{e(h)}^2}\right)^{1/4}\frac{1}{\sqrt{2^{N_{1e(h)}}N_{1e(h)}!}}\exp\left(-\frac{1}{2}\frac{(x-x_{oe(h)})^2}{\widetilde{L}_{e(h)}^2}\right)H_{N_{1e(h)}}\left(\frac{x-x_{oe(h)}}{\widetilde{L}_{e(h)}}\right) \tag{7}$$

$$\eta_{N_{2e(h)}}\left(\frac{z}{L_{e(h)}}\right)=\left(\frac{1}{\pi L_{e(h)}^2}\right)^{1/4}\frac{1}{\sqrt{2^{N_{2e(h)}}N_{2e(h)}!}}\exp\left(-\frac{1}{2}\frac{z^2}{L_{e(h)}^2}\right)H_{N_{2e(h)}}\left(\frac{z}{L_{e(h)}}\right) \tag{8}$$

where parameters

$$\widetilde{L}_{e(h)}=\sqrt{\frac{\hbar}{m_{e(h)}\widetilde{\omega}_{e(h)}}};\quad L_{e(h)}=\sqrt{\frac{\hbar}{m_{e(h)}\omega_{0e(h)}}}; \tag{9}$$

are the units of length.

$$H_n(\xi)=n!\sum_{k=0}^{[\frac{n}{2}]}\frac{(-1)^k}{k!(n-2k)!}(2\xi)^{n-2k} \tag{10}$$

is the Hermitian polynomial.

3. Preliminary relations

We start with the following general expression for the scattering cross-section $\frac{d^2S}{d\Omega d\nu}$ of the scattering of incident light with frequency ν_0 and polarization $\vec{e}_0$ into light with frequency ν_1 and polarization $\vec{e}_1$:

$$\frac{d^2S}{d\Omega d\nu} = \left(\frac{e^2}{m_0c^2}\right)^2 \frac{\nu_1}{\nu_0} \sum_{i,f} \left|A_{i,f}\right|^2 \hbar\delta(\hbar\nu - E_f + E_i) \tag{11}$$

where

$$A_{i,f} = \frac{1}{m_0} \sum_r \left(\frac{\langle f|\vec{e}_1\vec{p}|r\rangle\langle r|\vec{e}_0\vec{p}|i\rangle}{E_f - E_r + \hbar\nu_0} + \frac{\langle f|\vec{e}_0\vec{p}|r\rangle\langle r|\vec{e}_1\vec{p}|i\rangle}{E_f - E_r - \hbar\nu_1} \right) \tag{12}$$

Here *i*, *r* and *f* denote the initial, intermediate, and final states, respectively, E_i, E_r and E_f- are the corresponding energies, $\vec{p}$ is the one-electron momentum operator and m_0 is the free electron mass. $\nu = \nu_0 - \nu_1$ is a frequency shift. Equations (1) and (2) are based on the electric dipole approximation. The δ-function in (1) express the energy-conservation condition

$$\hbar\nu_0 = \hbar\nu_1 + E_f - E_i \tag{13}$$

Then Raman scattering processes consist of two steps. First, an incident light quantum is absorbed creating an electron –hole pair between the state (N_{1h}, N_{2h}) in the valence band and the state (N'_{1e}, N'_{2e}) in the conduction band. Second, a scattered photon is emitted due to an electronic transition from the state (N'_{1e}, N'_{2e}) to the state (N_{1e}, N_{2e}) in conduction band. The Raman shift $\hbar\nu$ is equal to the excitation energy of the electron-hole pair created in the scattering process.

In our model we assume that the conduction band is empty and the valence band completely occupied by electrons. We neglect all the transitions assisted by phonons.

The initial, intermediate and final state energy and wave functions are:

$$\begin{aligned}
E_i &= E_h(N_{1h}, N_{2h}, k_{yh}); \quad & \left|N_{1h}, N_{2h}, k_{yh}\right\rangle &= U_v\psi(N_{1h}, N_{2h}, k_{yh}) \\
E_r &= E'_e(N'_{1e}, N'_{2e}, k'_{ye}); \quad & \left|N'_{1e}, N'_{2e}, k'_{ye}\right\rangle &= U_c\psi(N'_{1e}, N'_{2e}, k'_{ye}) \\
E_f &= E_e(N_{1e}, N_{2e}, k_{ye}); \quad & \left|N_{1e}, N_{2e}, k_{ye}\right\rangle &= U_v\psi(N_{1h}, N_{2h}, k_{yh})
\end{aligned} \tag{14}$$

4. Calculation of Raman scattering cross section

Using Eqs. (14) the DCS for ERS can be written as

$$\begin{aligned}
\frac{d^2S}{d\Omega d\nu} = \left(\frac{e^2}{m_0c^2}\right)^2 \frac{\nu_0 - \nu}{\nu_0} \sum_{N_{1e}, N_{2e}} \sum_{N_{1h}, N_{2h}} \sum_{k_{ye}, k_{yh}} \left|A_{N_{1h}, N_{2e}, N_{1e}, N_{2e}}\right|^2 \hbar \cdot \delta\Big(\hbar\nu - E_g - \\
- E_{N_{1h}} - E_{N_{2h}} - E_{N_{1e}} - E_{N_{2e}} - \frac{\hbar^2 k_{ye}^2}{2m_e}\left(\frac{\omega_{0e}}{\tilde{\omega}_e}\right)^2 - \frac{\hbar^2 k_{yh}^2}{2m_h}\left(\frac{\omega_{0h}}{\tilde{\omega}_h}\right)^2\Big)
\end{aligned} \tag{15}$$

where

$$\begin{aligned}
A_{N_{1h}, N_{2e}, N_{1e}, N_{2e}} = \frac{1}{m_0} \sum_{N'_{1e}, N'_{2e}} \Bigg(\frac{\langle N_{1e}, N_{2e}, k_{ye} \left|\vec{e}_1\vec{p}\right| N'_{1e}, N'_{2e}, k'_{ye}\rangle\langle N'_{1e}, N'_{2e}, k'_{ye} \left|\vec{e}_0\vec{p}\right| N_{1h}, N_{2h}, k_{yh}\rangle}{E_h(N_{1h}, N_{2h}, k_{yh}) + \hbar\nu_0 - E'_e(N'_{1e}, N'_{2e}, k'_{ye})} + \\
+ \frac{\langle N_{1e}, N_{2e}, k_{ye} \left|\vec{e}_0\vec{p}\right| N'_{1e}, N'_{2e}, k'_{ye}\rangle\langle N'_{1e}, N'_{2e}, k'_{ye} \left|\vec{e}_1\vec{p}\right| N_{1h}, N_{2h}, k_{yh}\rangle}{E_h(N_{1h}, N_{2h}, k_{yh}) - \hbar(\nu_0 - \nu) - E'_e(N'_{1e}, N'_{2e}, k'_{ye})}
\end{aligned} \tag{16}$$

and

$$E_{N_{1e(h)}} = \left(N_{1e(h)} + \frac{1}{2} \right) \hbar \widetilde{\omega}_{e(h)}; \qquad E_{N_{2e(h)}} = \left(N_{2e(h)} + \frac{1}{2} \right) \hbar \omega_{0e(h)}; \tag{17}$$

The matrix elements of the interband transitions can be written as

$$\begin{aligned} \left\langle N_{1e},\, N_{2e},\, k_{ye} \left| \vec{e}_j \vec{p} \right| N'_{1e},\, N'_{2e},\, k'_{ye} \right\rangle &= \left\langle N_{1e},\, N_{2e},\, k_{ye} \left| e_{jx} p_x \right| N'_{1e},\, N'_{2e},\, k'_{ye} \right\rangle + \\ \left\langle N_{1e},\, N_{2e},\, k_{ye} \left| e_{jy} p_y \right| N'_{1e},\, N'_{2e},\, k'_{ye} \right\rangle &+ \left\langle N_{1e},\, N_{2e},\, k_{ye} \left| e_{jz} p_z \right| N'_{1e},\, N'_{2e},\, k'_{ye} \right\rangle \end{aligned} \tag{18}$$

where

$$\left\langle N_{1e},\, N_{2e},\, k_{ye} \left| e_{jx} p_x \right| N'_{1e},\, N'_{2e},\, k'_{ye} \right\rangle = - \frac{i\hbar}{\widetilde{L}_e} e_{jx} \delta_{N'_{2e}, N_{2e}} \left[\sqrt{\frac{N_{1e}}{2}} \delta_{N'_{1e}, N_{1e}-1} \sqrt{\frac{N_{1e}+1}{2}} \delta_{N'_{1e}, N_{1e}+1} \right] \delta_{k_{ye}, k'_{ye}} \tag{19}$$

$$\left\langle N_{1e},\, N_{2e},\, k_{ye} \left| e_{jy} p_y \right| N'_{1e},\, N'_{2e},\, k'_{ye} \right\rangle = \hbar k'_{ye} e_{jy} \delta_{N'_{2e}, N_{2e}} \delta_{N'_{1e}, N_{1e}} \delta_{k_{ye}, k'_{ye}} \tag{20}$$

$$\left\langle N_{1e},\, N_{2e},\, k_{ye} \left| e_{jz} p_z \right| N'_{1e},\, N'_{2e},\, k'_{ye} \right\rangle = - \frac{i\hbar}{L_e} e_{jz} \delta_{N'_{1e}, N_{1e}} \left[\sqrt{\frac{N_{2e}}{2}} \delta_{N'_{2e}, N_{2e}-1} - \sqrt{\frac{N_{2e}+1}{2}} \delta_{N'_{2e}, N_{2e}+1} \right] \delta_{k_{ye}, k'_{ye}} \tag{21}$$

If we consider allowed electron transitions between conduction and valence bands, the interband matrix element in the envelope function approximation, can be written as

$$\left\langle N'_{1e},\, N'_{2e},\, k'_{ye} \left| \vec{e}_j \vec{p} \right| N_{1h},\, N_{2h},\, k_{yh} \right\rangle = \left(\vec{p}_{cv} \cdot \vec{e}_j \right) \cdot I_{N_{1h}, N'_{1e}}(k_y) \cdot I_{N_{2h}, N'_{2e}} \cdot \delta_{k_{yh}, k'_{ye}} \tag{22}$$

where $\vec{p}_{cv} = \left\langle u_c \left| \vec{p} \right| u_v \right\rangle$ - the momentum matrix element between the valence and conduction bands (evaluated at $\vec{k} = 0$)and

$$I_{N_{1h}, N'_{1e}}(k_y) = \int_{-\infty}^{+\infty} \varphi_{N_{1h}} \left(\frac{x - x_{0h}}{\widetilde{L}_h} \right) \varphi_{N'_{1e}} \left(\frac{x - x_{0e}}{\widetilde{L}_e} \right) dx \tag{23}$$

$$I_{N_{2h}, N'_{2e}} = \int_{-\infty}^{+\infty} \eta_{N_{2h}} \left(\frac{z}{L_h} \right) \eta_{N'_{2e}} \left(\frac{z}{L_e} \right) dz \tag{24}$$

We find that the matrix elements (19)-(22) vanish unless the following selection rule is obeyed

$$k_{ye} = k_{yh} = k'_{ye} = k_y \tag{25}$$

The EHP does not change its total momentum during the absorption or the emission of a photon (photon momentum is neglected).

Using (10) it can be obtained that

$$\begin{aligned} I_{N_{1h}, N'_{1e}}(k_y) = {} & \left(\frac{1}{\pi} \right)^{1/2} \left(\frac{1}{\widetilde{L}_h \widetilde{L}_e} \right)^{1/2} \frac{N'_{1e}!\, N_{1h}!}{\sqrt{2^{N_{1e}+N_{1h}} N_{1e}!\, N_{1h}!}} \sum_{k=0}^{[N_{1h}/2]} \sum_{j=0}^{[N'_{1e}/2]} \frac{(-1)^{k+j} 2^{N_{1h}+N'_{1e}-2k-2j}}{k!\, j!\, (N_{1h}-2k)!\, (N'_{1e}-2j)!} \left(\frac{1}{\widetilde{L}_e} \right)^{N'_{1e}-2j} \cdot \\ & \cdot \left(\frac{1}{\widetilde{L}_h} \right)^{N_{1h}-2k} \sum_{\mu=0}^{N_{1h}-2k} \frac{(N_{1h}-2k)!}{\mu!\, (N_{1h}-2k-\mu)!} (x_{0e} - x_{0h})^{N_{1h}-2k-\mu} \sum_{\nu=0}^{N'_{1e}-2j+\mu} \frac{(N'_{1e}-2j+\mu)!}{\nu!\, (N'_{1e}-2j+\mu-\nu)!} \cdot \\ & \cdot \left[(-1)^{\nu} + 1 \right] exp\left(- \frac{(x_{0e} - x_{0h})^2}{2(\widetilde{L}_e^2 + \widetilde{L}_h^2)} \right) \frac{1}{2} \left(\frac{\widetilde{L}_e^2 + \widetilde{L}_h^2}{2\widetilde{L}_e^2 \widetilde{L}_h^2} \right)^{-\frac{\nu+1}{2}} \Gamma\left(\frac{\nu+1}{2} \right) \left(- \frac{\widetilde{L}_e^2 (x_{0e} - x_{0h})}{\widetilde{L}_e^2 + \widetilde{L}_h^2} \right)^{N'_{1e}-2j+\mu-\nu} \end{aligned} \tag{26}$$

and

$$I_{N_{2h},N'_{2e}} = \left(\frac{1}{\pi}\right)^{1/2} \frac{1}{\sqrt{L_e L_h}} \sqrt{\frac{N_{2h}!\, N'_{2e}!}{2^{N_{3e}+N_{3h}}}} \sum_{\alpha=0}^{[N'_{2e}/2]} \sum_{\beta=0}^{[N_{3h}/2]} \frac{(-1)^{\alpha+\beta} 2^{N'_{2e}-2\alpha+N_{3h}-2\beta}}{\alpha!\,\beta!\,(N'_{2e}-2\alpha)!\,(N_{3h}-2\beta)!} \cdot$$

$$\cdot \left(\frac{1}{L_e}\right)^{N'_{2e}-2\alpha} \left(\frac{1}{L_h}\right)^{N_{3h}-2\beta} \left[(-1)^{N'_{2e}+N_{3h}-2\alpha-2\beta}+1\right] \frac{\Gamma\left(\frac{N'_{2e}+N_{3h}-2\alpha-2\beta+1}{2}\right)}{2\left(\frac{\sqrt{L_h^2+L_e^2}}{\sqrt{2}L_h L_e}\right)^{N'_{2e}+N_{3h}-2\alpha-2\beta+1}} \tag{27}$$

X-X scattering

We first consider the case where both the incident and the scattered radiation are polarized parallel to the x axis.

Performing the summation over k_y in (15) we obtain expression for DCS of the ERS process:

$$\frac{d^2S^{xx}}{d\Omega d\nu} = \sigma_0 \frac{\nu_0-\nu}{\nu_0} \sum_{N_{1h},N_{2h},N_{1e},N_{2e}} \left[\sum_{N'_{1e},N'_{2e}} I_{N_{1h},N'_{1e}}\left(k_y(\nu)\right)\cdot I_{N_{2h},N'_{2e}} \cdot \delta_{N'_{2e},N_{2e}} \cdot \left(\sqrt{\frac{N_{1e}}{2}}\cdot\delta_{N'_{1e},N_{1e}-1} -\right.\right.$$

$$\left.\left. - \sqrt{\frac{N_{1e}+1}{2}}\cdot\delta_{N'_{1e},N_{1e}+1}\right)\cdot\left(\frac{1}{A(\nu)}+\frac{1}{B(\nu)}\right)\right]^2 \cdot \frac{1}{\sqrt{\frac{\hbar\nu}{E_g}-\frac{E_{N_{1e}}}{E_g}-\frac{E_{N_{1h}}}{E_g}-\frac{E_{N_{2e}}}{E_g}-\frac{E_{N_{2h}}}{E_g}-1}} \tag{28}$$

where

$$\sigma_0 = \left(\frac{e^2}{m_0c^2}\right)^2 \frac{L_y|\vec{p}_{cv}|^2\hbar^2}{\sqrt{2}\pi\tilde{L}_e^2 m_0^2 E_g^{5/2}\sqrt{\frac{1}{m_e}\left(\frac{\omega_{0e}}{\tilde{\omega}_e}\right)^2+\frac{1}{m_h}\left(\frac{\omega_{0h}}{\tilde{\omega}_h}\right)^2}} \tag{29}$$

$$A(\nu) = \frac{\hbar}{E_g}\left(\nu_0-\nu+(N_{2e}-N'_{2e})\omega_{0e}+(N_{1e}-N'_{1e})\tilde{\omega}_e\right) \tag{30}$$

$$B(\nu) = \frac{\hbar}{E_g}\left((N_{2e}-N'_{2e})\omega_{0e}+(N_{1e}-N'_{1e})\tilde{\omega}_e-\nu_0\right) \tag{31}$$

and $k_y(\nu)$ -is the root of the delta function argument

$$|k_y(\nu)| = \frac{\sqrt{2}}{\hbar}\frac{\left(\hbar\nu-E_g-E_{N_{1e}}-E_{N_{1h}}-E_{N_{2e}}-E_{N_{2h}}\right)^{\frac{1}{2}}}{\sqrt{\frac{1}{m_e}\left(\frac{\omega_{0e}}{\tilde{\omega}_e}\right)^2+\frac{1}{m_h}\left(\frac{\omega_{0h}}{\tilde{\omega}_h}\right)^2}} \tag{32}$$

Z-Z Scattering

We next display the Raman cross section for the case where the incident and scattered light are polarized parallel to z axis:

$$\frac{d^2S^{zz}}{d\Omega d\nu} = \sigma_1 \frac{\nu_0-\nu}{\nu_0} \sum_{N_{1h},N_{2h},N_{1e},N_{2e}} \left[\sum_{N'_{1e},N'_{2e}} I_{N_{1h},N'_{1e}}\left(k_y(\nu)\right)\cdot I_{N_{2h},N'_{2e}} \cdot \delta_{N'_{1e},N_{1e}} \cdot \left(\sqrt{\frac{N_{2e}}{2}}\cdot\delta_{N'_{2e},N_{2e}-1} -\right.\right.$$

$$- \sqrt{\frac{N_{2e}+1}{2}} \cdot \delta_{N'_{2e},N_{2e}+1} \Bigg) \cdot \left(\frac{1}{A(\nu)} + \frac{1}{B(\nu)} \right) \Bigg]^2 \cdot \frac{1}{\sqrt{\frac{\hbar\nu}{E_g} - \frac{E_{N_{1e}}}{E_g} - \frac{E_{N_{1h}}}{E_g} - \frac{E_{N_{2e}}}{E_g} - \frac{E_{N_{2h}}}{E_g} - 1}} \quad (33)$$

where

$$\sigma_1 = \left(\frac{e^2}{m_0 c^2} \right)^2 \frac{L_y |\vec{p}_{cv}|^2 \hbar^2}{\sqrt{2}\pi L_e^2 m_0^2 E_g^{5/2} \sqrt{\frac{1}{m_e}\left(\frac{\omega_{0e}}{\tilde{\omega}_e}\right)^2 + \frac{1}{m_h}\left(\frac{\omega_{0h}}{\tilde{\omega}_h}\right)^2}} \quad (34)$$

Let us make some remarks concerning the above equations. From Eq.(27) it follows that $I_{N_{2h},N'_{2e}}$ vanishes unless $N'_{2e} + N_{2h} = 2n$, where n is an integer. So, transition can only take place between N_{2h} and N'_{2e} subbands with the same parity ($2m \to 2n$; and $2m+1 \to 2n+1$; m and n are integers). But for Eq. (26) quantum numbers N_{1h} and N'_{1e} can change arbitrarily.
Hence, the following selection rules are obtained for interband transitions:

$$\left| N_{1h} - N'_{1e} \right| = 0,1,2,....;$$
$$\left| N_{2h} - N'_{2e} \right| = 0,2,4...$$

As can be seen from Eqs. (28) and (33) the DCS is directly proportional to the density-of –states of carriers in the valence and conduction bands and the interband matrix elements. In this case, the scattering spectrum shows density-of-states peaks and interband matrix elements maximums. The positions of these structures are given as follows:

$$\hbar\nu = E_{N_{1h}} + E_{N_{2h}} + E_{N_{1e}} + E_{N_{2e}} + E_g \quad (35)$$

Here, the following selection rules must be fulfilled: $N'_{1e} = N_{1e} \pm 1$, $N'_{2e} = N_{2e}$ for X-X polarization and $N'_{2e} = N_{2e} \pm 1$, $N'_{1e} = N_{1e}$ for Z-Z polarization. In this case when $\left| N_{1h} - N'_{1e} \right| = 2n+1$ the spectrum shows maximums and when $\left| N_{1h} - N'_{1e} \right| = 2n$ the ERS spectrum shows singular peaks. The peaks and maximums related to these structures correspond to interband EHP transition and their position depends on the magnetic field.

Other singularities of equations (28) and (33) occur whenever $A(\nu) = 0$. In the X-X scattering configuration this singularity is

$$\hbar\nu = \hbar\nu_0 - \hbar\tilde{\omega}_e \quad (36)$$

Here the following selection rules is fulfilled: $N'_{1e} = N_{1e} + 1$, $N'_{2e} = N_{2e}$.

For Z-Z scattering configuration Raman singularity is

$$\hbar\nu = \hbar\nu_0 - \hbar\omega_{0e} \quad (37)$$

In this case the selection rules are $N'_{1e} = N_{1e}$,

$$N'_{2e} = N_{2e} + 1.$$

As can be seen from equations (36) and (37) these frequencies correspond to electron transitions connecting the subband edges for a process involving the conduction band (i.e., intraband transitions).
We can also notice that Y-Y scattering configuration is free from Raman singularity and related to selection rules $N'_{1e} = N_{1e}$, $N'_{2e} = N_{2e}$.

5. Discussion of the results

In the following we present detailed numerical calculations of DCS of GaAs/AlGaAs parabolic quantum wire in the presence of uniform magnetic field as a function $\hbar\nu / E_g$. The physical parameters used in our expressions are: $E_g = 1.5177$ eV, $m_e = 0.0665 m_0$, $m_h = 0.45 m_0$ (the heave-hole band). Taking the ratio 60:40 for the band-edge discontinuity [20, 21], the conduction and valence barrier heights are taken to be $\Delta_e = 255$ meV and $\Delta_h = 170$ meV. The oscillation frequencies ω_{0e} and ω_{0h} of the parabolic quantum wire are determined via

$$\omega_{0e(h)} = \frac{2}{d}\sqrt{\frac{2\Delta_{e(h)}}{m_{e(h)}}}$$

where d -is the quantum wire diameter.
In figure 1 (a)-1(d) we show the Raman spectra of the parabolic quantum wire in the X-X scattering configuration for different magnetic fields, such as $H = 0, 2\cdot10^4, 6.5\cdot10^4, 8.5\cdot10^4$ Gauss. The diameter d of the QWR is 2000 $\overset{o}{A}$. The incident radiation frequency was fixed as $\hbar\nu_0 = 1.82$ eV. The positions of the singularities are defined by (35) and (36).

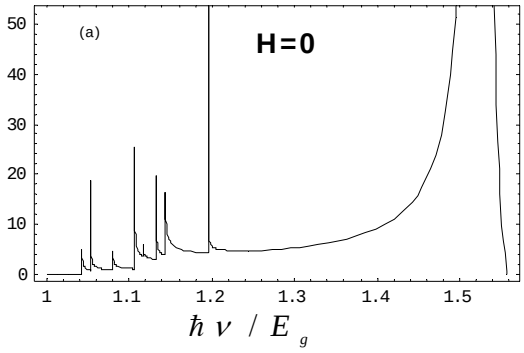

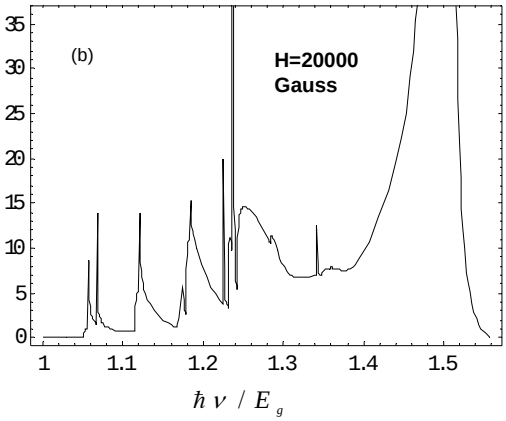

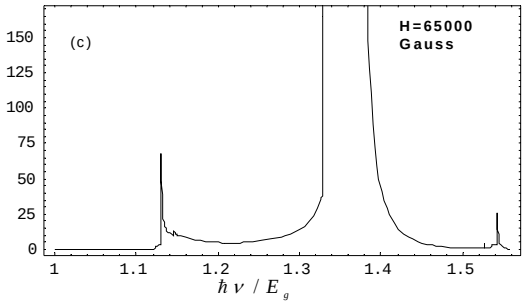

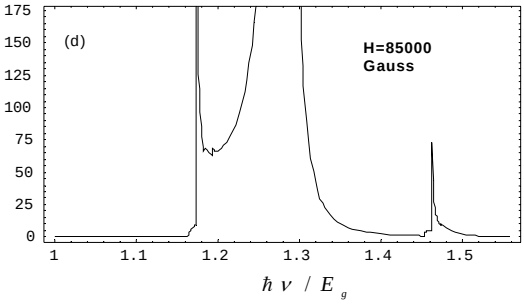

Fig. 1 (a)-(d). Calculated Raman cross section of the PQWR in the X-X scattering configuration with different transverse magnetic field.

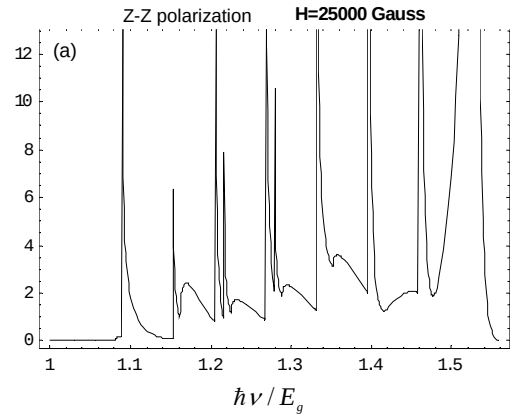

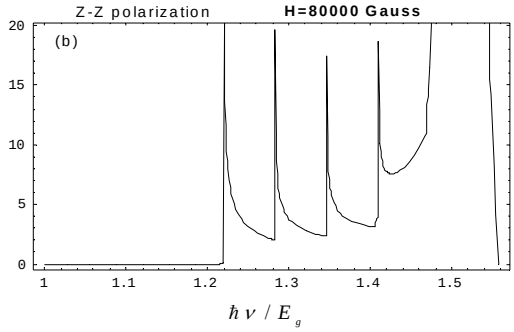

Fig.2 (a)-(b). Calculated Raman cross section of the PQWR in the Z-Z scattering configuration with different transverse magnetic field.

Fig.2(a)-2(b) shows Raman spectra for Z-Z scattering configuration for magnetic fields H=2.5·10^4, 8·10^4, Gauss. The other parameters coincide with those of figure 1.

The structure of the DCS, as given in the figures provides a transparent understanding of the energy subband structure of the parabolic quantum wire in a transverse magnetic field.

In the present work we have applied a simplified model for the electronic structure of the system. In a more realistic case we should consider multiband structure using a calculation model like that of Luttinger-Kohn or the Kane model. The above-mentioned assumptions would lead to better results but entail more complicated calculations. However, within the limit of our simple model we are able to account for the essential physical properties of the discussed problem. The fundamental features of the DCS, as described in our paper, should not change very much in real QWR case. It can be easily proved that the singular peak in the DCS will be present irrespective of the model used for the subband structure and may be determined for the values of $\hbar\nu_1$ equal to the energy difference between two subbands $\hbar\nu_1 = \hbar\nu_0 - \hbar\nu = E^e_\alpha - E^e_\beta$ where $E^e_\alpha > E^e_\beta$ are respective electron energies in the subbands. At present there is a lack of experimental work on this type of ERS. Our major aim in performing these calculations is to stimulate experimental research in this direction.

[1] *Y. Nagamune, Y. Arakawa, S. Tsukamoto, M. Nishioika, S. Sasaki and M. Miura*. Phys. Rev. Lett., 1992, 69 2963.
[2] *A.S. Plaut, H. Lage, P. Grambow, D. Heitmann, von Klitzing K. and K. Ploog. Phys. Rev. Lett.*, 1991, 67 1642.
[3] *T. Demel, D. Heitmann, P. Grambow and K. Ploog*. Phys. Rev. Lett., 1991,66 2657.
[4] *A.R. Goni, A. Pinczuk, J.S. Weiner, B.S. Dennis, L.N. Pfeifer and K.W. West*. Phys. Rev. Lett. 1991, 70 1151.
[5] *K.K. Choi, D.C. Tsui and S.C. Palmateer*. Phys. Rev., 1986, B 33 8216.
[6] *C.J.B. Ford, T.J. Thornton, R. Newbery, M. Pepper, H. Ahmed, G. Davies and D. Andrews*. Superlatt. Microstruct, 1988, 4 451.
[7] *J. Liu , K. Ismail , K.Y. Lee, J.M. Hong and S. Washburn*. Phys. Rev., 1993, B 47 13039.
[8] *J.A. Brum, G. Bastard, L.L. Chang and L. Esaki.* Superlatt. Microstruct, 1997 3 47.
[9] *G. Bastard, J.A. Brum and R. Ferreira*. Solid State Phys., 1991, 44 395.
[10] *A. Lorenzoni and L.C. Andreani*. Semicond. Sci. Technol., 1999, 14 1169.
[11] *M. Cardona and G. Güntherodt*. 1989 Light Scattering in Solids V (Topics in Applied Physics 66) (Heidelberg: Springer).
[12] *M. Cardona*. Superlatt. Microstruct, 1990, 7 183.
[13] *A. Pinczuk and E. Burstein.* 1983 Light Scattering in Solids I (Springer Topics in Applied Physics 8) ed. M. Cardona (Heidelberg: Springer).
[14] *R.F. Wallis and D.L. Mills*. Phys. Rev. B, 1970, 2 3312.
[15] *F. Comas, C. Trallero-Giner., I.G. Lang. and S.T. Pavlov.* 1985 Fiz. Tverd. Tela 27 57 (Engl.Transl. Sov. Phys. Solid State 27 32).
[16] *F. Bechstedt, R. Enderlein and K. Peuker*. Phys. Status Solidi (b), 1975, 68 43
[17] *R. Riera, F. Comas, C. Trallero-Giner and S.T. Pavlov*. Phys. Status Solidi (b), 1988, 148 533.
[18] *R. Betancourt-Riera, J.M. Bergues, R. Riera, J.L. Marin*. Physica, 2000, E 5 204.
[19] *J.H. Burnett, H.M. Cheong, R.M. Westervelt, W. Paul, P.F. Hopkins, M. Sundaram, and A.C. Cossard.* Phys. Rev. B, 1993, 47 4524.
[20] *R.C. Miller, D.A. Kleinman, and A.C. Gossard.* Phys. Rev B, 1984, 29 7085.
[21] *J. Batey, S.L. Wright, and D.J. Di Maria*. J. Appl. Phys. 1985.57 484.

T.H. İsmayılov, B.H. Mehdiyev

MAQNİT SAHƏSİNDƏ YERLƏŞMİŞ KVANT MƏFTİLİNDƏ RAMAN SƏPİLMƏSİ

Eninə magnit sahəsində yerləşmiş parabolic kvant məftilində fononun iştirakı olmadan işığın Raman səpilməsi tədqiq edilmişdir. Elektron Raman səpilməsinin effektiv en kəsiyinin tezliyin sürüşməsindən və maqnit sahəsindən asılılığı hesablanmışdır. Kvantlanmış alt səviyyələr arasında zonalararası və zonadaxili keçidlərin iştirakı ilə baş verən proseslərə baxılmışdır. Düshən və səpilən işığin polyarizasiyasından asılı olaraq secmə qaydaları məsələnin müxtəlif parametrlərinin (siklotron tezlikləri və saxlayicı potencilın tezliyi) qiymətlərində tədqiq edilmişdir. Electron Raman səpilməsinin differensial effectiv en kəsiyi hal sıxlığı ilə bağlı məxsusiyyətlərə və keçidlərin matris elementləri ilə bağlı əlavə strukturlara malikdir.

Т.Г. Исмаилов, Б.Г. Мехтиев

ЭЛЕКТРОННОЕ КОМБИНАЦИОННОЕ РАССЕЯНИЕ СВЕТА В КВАНТОВОЙ ПРОВОЛОКЕ В МАГНИТНОМ ПОЛЕ

Исследовано электронное комбинационное рассеяние света (ЭКРС), без участия фононов, в параболической квантовой проволоке ,в поперечном магнитном поле . Рассчитаны зависимости сечения ЭКРС от сдвига частоты и магнитного поля. Рассмотрены процессы с участием как межзонных, так и внутризонных преходов между квантованными подзонами. Изучены правила отбора и проведен анализ дифференциального сечения рассеяния для различных поляризаций падающего и рассеянного излучений и для различных соотношений между параметрами задачи (циклотронными частотами и частотами удерживающего потенциала электронов и дырок). Сечение ЭКРС содержит сингулярности обязанные плотности состояний и дополнительные структуры ,связанные с матричными элементами переходов.

Received: 22.06.04.